Seismic Determination of Elastic Anisotropy and Mantle Flow

Jeffrey Park; Yang Yu

Science, New Series, Vol. 261, No. 5125 (Aug. 27, 1993), 1159-1162.

Stable URL:
http://links.jstor.org/sici?sici=0036-8075%2819930827%293%3A261%3A5125%3C1159%3ASDOEAA%3E2.0.CO%3B2-7

Science is currently published by American Association for the Advancement of Science.

Seismic Determination of Elastic Anisotropy and Mantle Flow

Jeffrey Park and Yang Yu

When deformed, many rocks develop anisotropic elastic properties. On many seismic records, a long-period (100 to 250 seconds), "quasi-Love" wave with elliptical polarization arrives slightly after the Love wave but before the Rayleigh wave. Mantle anisotropy is sufficient to explain these observations qualitatively as long as the "fast" axis of symmetry is approximately horizontal. Quasi-Love observations for several propagation paths near Pacific Ocean subduction zones are consistent with either flow variations in the mantle within or beneath subducting plates or variations in the direction of fossil spreading in older parts of the Pacific plate.

Plastic flow in the Earth's upper mantle is thought to cause the preferred orientation of olivine and orthopyroxene, two of the major components of peridotite. If lateral variations in this anisotropy can be detected and located, we can identify deformations of the mantle associated with both past and present plate motions and orogenic episodes (*1*). When this information is combined with information from seismic tomography and earthquake source studies, mantle processes that underlie plate tectonic motions can be revealed. Love waves are progressively converted to Rayleigh-polarized motion (and vice versa) as a surface wave travels through lateral gradients of anisotropy. We call this converted wave packet a "quasi-Love" wave. The details of the quasi-Love wave are determined by a horizontal integral of anisotropic properties along the wave path, which complements the vertical integral offered by observations of shear-wave splitting (*1, 2*).

Theoretical calculations have shown that Rayleigh and Love surface waves interact in the presence of seismic anisotropy (*3–5*). We have previously modeled Rayleigh-Love interaction in anisotropic structures at long periods ($\gtrsim$100 s) (*6, 7*); our calculations were performed with seismic free oscillations, the normal vibrational modes of the whole Earth, rather than with traveling waves (*8–10*). Toroidal modes sum to form Love waves on the transverse-horizontal component of particle motion. Spheroidal modes sum to form Rayleigh waves on the vertical and radial-horizontal components. Strong spheroidal-toroidal coupling breaks down this separation: quasi-Love waves appear on the vertical and radial-horizontal components of motion, normally the reserve of spheroidal motion. Likewise, hybrid spheroidal modes sum to form quasi-Rayleigh waves on the transverse component. Anisotropy with a horizontal axis of symmetry generates these waveform anomalies more readily than do lateral variations in isotropic *S*- and *P*-wave velocities, topography on model boundaries, or anisotropy with a vertical axis of symmetry (*7*).

In practice, shallow strike-slip earthquakes are ideal for the study of Rayleigh-Love interaction: quasi-Rayleigh waves are evident at the Love wave radiation minima, and quasi-Love waves are evident at the Rayleigh wave radiation minima. Because long period surface waves can refract by 10° or more (*11*), one must distinguish a quasi-Rayleigh wave from the transverse component of a refracted Rayleigh wave. Love waves cannot be refracted onto the vertical component; therefore, quasi-Love waves are easier to identify. At periods (T) $\gtrsim$100 s, the arrival windows of dispersed Rayleigh waves and quasi-Love waves differ significantly, aiding discrimination.

For an example, we present here low-passed seismic records from the 28 June 1992 strike-slip Landers, California, earthquake [surface-wave magnitude (M_S) = 7.5] recorded at stations SNZO (South Karori, New Zealand) and CTAO (Charters Towers, Australia) (Fig. 1). Paths to these stations issue from the Landers source near the auxiliary plane of the earthquake double-couple source mechanism, where the ratio of Love to Rayleigh radiation is large (*12*). The CTAO record is similar to a synthetic seismogram from a spherical reference model: the Love wave dominates, a weak Rayleigh wave follows, and little motion precedes the Rayleigh wave packet on the vertical component. In contrast, a strong precursor to the Rayleigh wave is seen on the SNZO record. The precursor is Rayleigh-polarized, with a 90° phase lag between the vertical and radial components of particle motion. We identify this anomaly as a coupled-mode quasi-Love wave.

The paths from the Landers event to CTAO and SNZO both cross the central Pacific (Fig. 2). The path to CTAO passes closer to Hawaii. Surface waves to CTAO cross the boundary between the Pacific and Indo-Australian plates, marked by the Solomon Islands, where the relative plate motion is largely transcurrent. The last 3000 km of the path to SNZO lies west of and subparallel to the Tonga-Kermadec subduction zone. The Landers event is not unique; we have identified similar quasi-Love waveform anomalies on several SNZO records from strike-slip earthquakes in California, such as the first large aftershock (M_S = 6.0) of the 26 April 1992 earthquake sequence near Eureka, California. In all cases, quasi-Love waveforms followed the main Love wave packet closely. This relation suggests that the Love waves converted partially to Rayleigh waves close to the receiver.

We considered three seismotectonic mechanisms for the generation of the quasi-Love waveforms observed at SNZO: (i) a sharp lateral interface in isotropic seismic velocities associated with the cold subducting slab; (ii) a sea-floor corrugation in the form of a single sine wave, with a wavelength of 200 km and 10-km peak-to-peak relief, to represent the Kermadec arc-trench topography; and (iii) a sharp transition from deformed to undeformed peridotite with a horizontal symmetry axis perpendicular to the trench. The third model represents the effect of the Pacific plate losing its fossil anisotropy, or at least its horizontal orientation, as it subducts at the trench. The spherical reference seismic velocity model we used was the oceanic PEM (*13*), whose ocean layer is 3 km deep. The elasticity variations were fixed in a layer between the Moho (Mohorovičić discontinuity) and a depth of 220 km. In the model, we used a 45° spherical cap at both poles for the lateral structure. This assump-

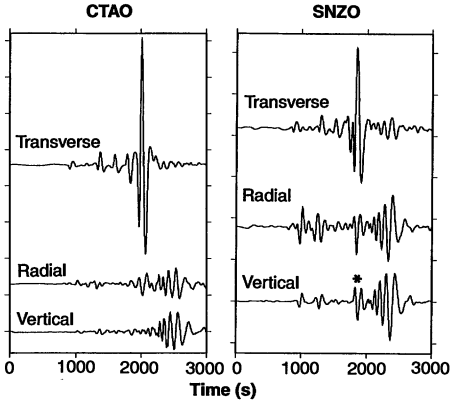

Fig. 1. Seismic data from the 28 June 1992 Landers, California, earthquake (M_S = 7.5) (*27*), recorded at observatories SNZO and CTAO. The data were low-pass filtered at 10 mHz (T = 100 s). The horizontal components are rotated to the radial and transverse components, parallel and normal, respectively, to the source-receiver great circle. The asterisk marks the quasi-Love waveform anomaly.

Department of Geology and Geophysics, Yale University, P.O. Box 6666, New Haven, CT 06511.

tion yields zonal symmetry and greatly simplifies the modal coupling calculations. The structure can be rotated so that the lateral discontinuity aligns with the Tonga-Kermadec subduction zone. The sea-floor corrugation is likewise centered at ±45°. The anisotropic variation was 6% in horizontal *P*-wave velocity (V_P), which is consistent with marine refraction data and the properties of deformed peridotite (*14*). The speed of the *P* wave varies with cos 2θ dependence, where θ is the angle between the propagation azimuth and the axis of symmetry. The sea-floor boundary perturbation breaches the free surface in the PEM model, but we expect that this will have a second-order effect on long-period, spheroidal-toroidal interaction.

We used the fundamental and the first four overtone dispersion branches to construct synthetic seismograms that were low-pass filtered at 100 s (frequency ≤10 mHz). Numerical experiments indicate that long-period quasi-Love waves are generated chiefly by interaction between the fundamental dispersion branches. The seismic source was fixed at a depth of 10 km and had a strike-slip mechanism. As shown in Fig. 3, a quasi-Love wave on the vertical component was associated only with the anisotropic model, although refraction of the Love wave onto the radial-horizontal component occurred for the isotropic model. Sea-floor topography and crustal structure strongly influence the surface waves at short periods ($T < 25$ s) (*15, 16*) but exert weak influence at the periods we considered. Extending the isotropic perturbation to a depth of 400 or 600 km had little effect. In other experiments, we found that it was very difficult to generate quasi-Love waveform anomalies without strong lateral gradients in anisotropy.

Comparison of data from SNZO with data generated from the models suggests that the lateral gradient does not coincide with the plate boundary but may lie at least 500 km east of it. Additional constraints can be found in other seismic records on independent propagation paths. The 4 November 1992 strike-slip event near the Balleny Islands (M_S = 6.3) offers near-nodal paths to stations CTAO, RAR (Rarotonga Island), GUMO (Guam), and MAJO (Matsushiro, Japan) (Fig. 4). The record at station RAR shows a clear precursor to the Rayleigh wave packet. Although the path did not cross a plate boundary, it crossed the New Zealand shelf and parallels the Tonga-Kermadec subduction zone on the side of the subducting plate. Weak or absent quasi-Love waveforms were seen at CTAO and GUMO, but strong coupled-mode anomalies appear on the MAJO record (Fig. 4). Surface waves from this earthquake propagated along the Marianas and Izu-Bonin subduction zones between GUMO and MAJO. We also examined a collection of shallow strike-slip events from western New Guinea to the Vanuatu Islands. The propagation paths to MAJO for these events traverse either the downgoing (Pacific plate) or overriding (Philippine plate) side of the Marianas–Izu-Bonin plate boundary. The records for paths confined to the Pacific plate exhibit strong quasi-Love precursors, but the records for paths on the Philippine plate do not. Quasi-Love anomalies are absent in data at SNZO from three strike-slip events on the southeast Indian Ridge. Therefore, anisotropic coupling is weak in the Indo-Australian plate at its boundary with the Pacific plate, at least southwest of SNZO as well as along the mid-ocean ridge.

The absence of quasi-Love waveforms for a source-receiver path does not require the absence of upper mantle anisotropy along that path. Surface waves that propagate parallel to the axis of symmetry experience weaker coupling effects (*3, 4*). Anisotropy with a vertical axis of symmetry couples spheroidal and toroidal free oscillation weakly, as does anisotropy with weak lateral variation. Anisotropy devel-

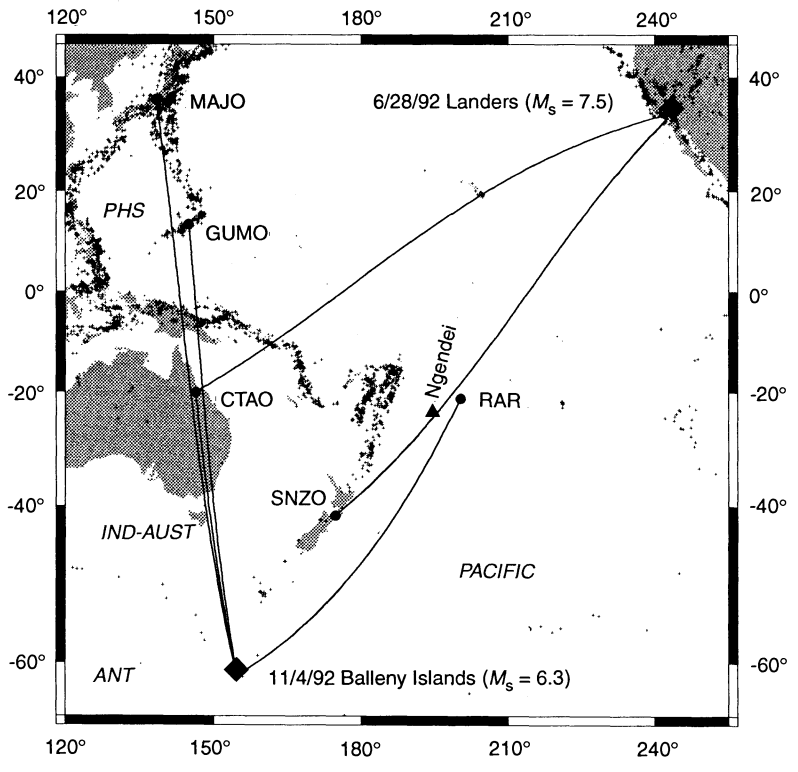

Fig. 2. Sources and receivers for the seismic data. The location of the 1983 Ngendei seismic refraction study is indicated. Also plotted are epicenters (from 1988 to 1991) (*27*) (small crosses); these earthquakes outline the plates bordering the Pacific plate on the west. *PHS*, Philippine Sea plate; *IND-AUST*, Indo-Australian plate; *ANT*, Antarctic plate. The intense seismic activity north of New Zealand is associated with the Tonga-Kermadec subduction zone.

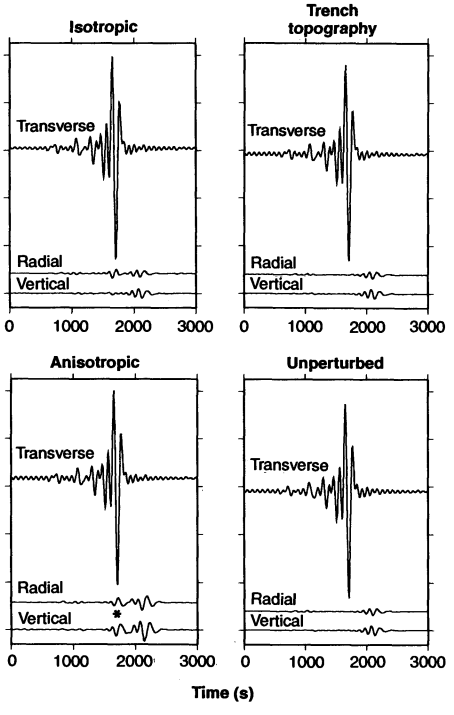

Fig. 3. Synthetic seismograms for Landers SNZO geometry. The lateral structure has zonal symmetry in all cases, with sharp lateral interfaces or sea-floor boundary corrugations along a small circle at 45° latitude, rotated to align with the Tonga-Kermadec trench. The effects of Earth rotation and ellipticity are omitted. The asterisk marks the quasi-Love waveform anomaly.

oped at ridge crests and transported with a large rigid plate could have weak lateral gradients. Similar to those in the Landers CTAO path, quasi-Love waveforms with $T \geq 125$ s are weak for the first surface waves of the 6 March 1988 Gulf of Alaska earthquake (M_S = 7.6), which was recorded at Geoscope station PPT (Papeete, Tahiti) (*7, 17*). Angular selection rules for modal coupling along the fundamental dispersion branch indicate that rough lateral structure generates waveform anomalies at higher frequencies than does smooth lateral structure (*6, 7*). A strong argument for sharp lateral gradients in anisotropy northwest of SNZO is that quasi-Love motion is manifest to a frequency of roughly 40 mHz (T = 25 s).

On the basis of recent tomographic studies (*2, 18*), researchers have inferred that azimuthal variations in long-period Rayleigh and Love phase velocity are 1 to 2% and that no anisotropy below the upper 200 km of the mantle is necessary to explain the data. Tomographic inversion for anisotropy is sensitive primarily to lateral structure with long wavelength, so a direct comparison with our observations is difficult. The arrival of quasi-Love waves before the second Rayleigh wave (R_2) is common in the global data set. These observations are consistent with smoothly varying anisotropy of a few percent in the upper 200 km of the mantle and therefore are also consistent with the tomographic models. However, some of the quasi-Love waves that arrive before R_1, such as those described here, require stronger anisotropic variations. Shear-wave anisotropy of a few percent in the upper mantle may contribute to the waveform anomalies, but numerical experiments demonstrate that the trade-off between P and S anisotropy is not simple. In a peridotite mantle, the ratio of V_P and V_S (S-wave velocity) anisotropy varies with the relative proportion of orthopyroxene and olivine (*19*), and thus this ratio could provide information on the bulk mineralogy of the mantle. Shear-wave anisotropy of a few percent in the upper 200 km of the mantle appears necessary to explain the splitting of SKS body waves, at least in many continental regions (*1, 20*).

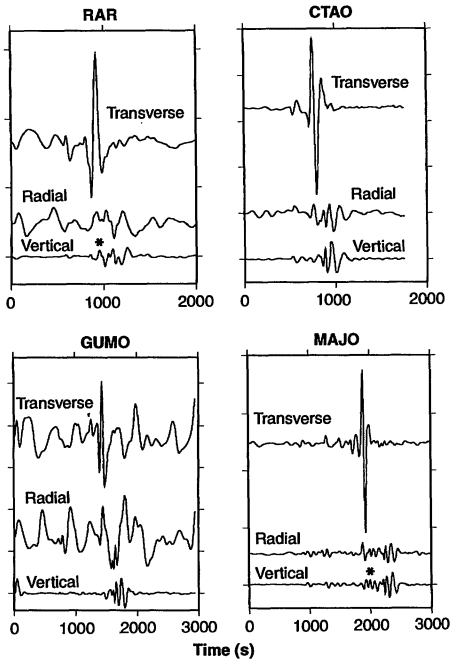

Fig. 4. Seismic data from the 4 November 1992 Balleny Islands earthquake (M_S = 6.3) (*27*), recorded at observatories CTAO, RAR, GUMO, and MAJO. The data were low-pass filtered at 10 mHz (T = 100 s). The horizontal components are rotated to the radial and transverse components, parallel and normal, respectively, to the source-receiver great circle. Significant long-period, horizontal component noise is evident at the ocean island stations RAR and GUMO. The asterisks mark quasi-Love waveform anomalies.

Careful modeling will be necessary to distinguish whether fossil or active mantle deformation is the cause of the anisotropic gradients required by the seismic data. The RAR record for the Balleny Islands event suggests that these gradients extend at least 1000 to 2000 km east of the plate boundary. Asthenospheric anisotropy could develop in the corner flow beneath the Pacific plate as it sinks into the mantle or as a result of the northward absolute motion of the Tonga-Kermadec subduction zone (*21, 22*). Lateral variations in the direction of fossil spreading, preserved in Mesozoic Pacific lithosphere, are also a possible cause. Magnetic anomaly patterns are not helpful for this portion of the Pacific plate, which was formed in the Cretaceous long interval of normal polarity. Fossil anisotropy in Mesozoic lithosphere may have been annealed or reset as the plate passed over the hot spot responsible for the Louisville Ridge, which lies across the path from California roughly 1000 km northwest of SNZO (*23*).

In numerical experiments, we can fit the Love and quasi-Love waveforms at SNZO with 6% P-wave anisotropy (in a depth range of 11 to 211 km) if the symmetry axis rotates from a west-northwest–east-southeast orientation to a north-northeast–south-southwest orientation at a sharp lateral boundary parallel to and roughly 500 km east of the Tonga-Kermadec trench. Although other models may fit the surface-wave data equally well, other data favor this 90° rotation of the direction of fossil spreading in this part of the Pacific plate. In the Ngendei seismic refraction survey (Fig. 2), Shearer and Orcutt (*24*) inferred that the sub-Moho mantle was anisotropic, with a fast axis aligned with N30°E. The symmetry axis predicted from extensions of the Eltanin and Menard fracture zones from the East Pacific Rise is northwest-southeast, perpendicular to the Ngendei axis. In a regional study of body wave travel times, Galea (*25*) inferred a N62°E symmetry axis for the Pacific plate near New Zealand, which is between these orientations. Comparison of SNZO data with data from the coupled-mode models, however, suggests that the conversion of Love waves to Rayleigh-polarized motion occurs much closer to SNZO than to the Ngendei field area. Therefore, the timing of the arrival of the quasi-Love wave relative to that of the Love wave favors either the model of northward asthenospheric shear east of the Tonga-Kermadec subduction zone or the hot spot reheating model (*26*).

REFERENCES AND NOTES

1. P. G. Silver and W. W. Chan, *Nature* **335**, 34 (1988).
2. Surface-wave tomography can also be used to investigate anisotropic structure [J.-P. Montagner and T. Tanimoto, *J. Geophys. Res.* **95**, 4797 (1990)]. However, the tomographic inverse problem suffers a large trade-off with lateral variation in isotropic seismic velocities. Long-period Rayleigh-Love interaction, by contrast, is only weakly sensitive to large-scale isotropic structure.
3. S. Kirkwood and S. Crampin, *Geophys. J. R. Astron. Soc.* **64**, 463 (1981).
4. ———, *ibid.*, p. 487.
5. V. Maupin, *Bull. Seismol. Soc. Am.* **80**, 1311 (1990).
6. J. Park and Y. Yu, *Geophys. J. Int.* **110**, 401 (1992).
7. Y. Yu and J. Park, *ibid.*, in press.
8. J. Park and F. Gilbert, *J. Geophys. Res.* **91**, 7241 (1986).
9. P. Lognonne, *ibid.* **96**, 20309 (1991).
10. V. Maupin, *Geophys. J.* **98**, 553 (1989).
11. A. Levshin, L. Ratnikova, J. Berger, *Bull. Seismol. Soc. Am.* **82**, 2464 (1992).
12. The Landers and Balleny Islands earthquakes have shallow (depth = 10 km) strike-slip mechanisms. The seismic data were obtained with the Gopher software of the data management system of the Incorporated Research Institutions for Seismology (IRIS). We have corrected the horizontal components at RAR for a 25° misalignment with true north and east.
13. A. M. Dziewonski, A. L. Hales, E. R. Lapwood, *Phys. Earth Planet. Inter.* **10**, 12 (1975).
14. A. Nicolas and N. I. Christensen, *Composition, Structure and Dynamics of the Lithosphere-Asthenosphere System* (Geodynamic Series, vol. 16, American Geophysical Union, Washington, DC, 1987).
15. K. L. McLaughlin, T. G. Barker, S. M. Day, B. Shkoller, J. L. Stevens, *Geophys. J. Int.* **111**, 291 (1992).
16. I. Nakanishi, *Geophys. Res. Lett.* **24**, 2385 (1992).
17. The quasi-Love wave at PPT appeared high-passed, with energy restricted to periods less than 100 to 120 s. Although the depth range of an anisotropic layer affects the frequency content of the quasi-Love wave, we failed to reproduce the behavior at PPT by varying the depth range and position of isolated sharp lateral gradients in anisotropic properties. However, we can generate high-passed, quasi-Love waves that resemble the PPT record by assuming a sinusoidally varying anisotropic structure with a wavelength of ≈2000 km. As the spacing between fracture zones that trend east and west in the northeast Pacific is roughly 1000 km, this is consistent with variations in the strength of fossil anisotropy acquired in different segments of the mid-Pacific ridge system.

18. C. E. Nishimura and D. W. Forsyth, *Geophys. J.* **96**, 203 (1989).
19. N. I. Christensen and S. M. Lundquist, *Bull. Geol. Soc. Am.* **93**, 279 (1982).
20. L. P. Vinnik, L. I. Makeyva, A. Milev, A. Y. Usenko, *Geophys. J. Int.* **111**, 433 (1992).
21. D. Giardini and J. H. Woodhouse, *Nature* **319**, 551 (1986).
22. K. M. Fischer, K. C. Creager, T. H. Jordan, *J. Geophys. Res.* **96**, 14403 (1991).
23. Recent experiments by N. M. Ribe and U. R. Christensen [*Eos* **73** (suppl.), 578 (1992)] with three-dimensional numerical convection models suggest that plumes do not penetrate the lithosphere to a great degree and so may not reset fossil anisotropy. However, large-scale lateral motion in the asthenosphere occurs in their calculations as the plume material spreads at the base of the lithosphere. Lateral gradients in anisotropic properties may exist near the Hawaii plume because quasi-Love waves, coeval with the Love wave, can be observed on several seismic records that approach station KIP (Kipapa, Hawaii) from the west.
24. P. M. Shearer and J. A. Orcutt, *Geophys. J. R. Astron. Soc.* **87**, 967 (1986).
25. P. Galea, *Phys. Earth Planet. Inter.* **76**, 229 (1993).
26. Shear in the asthenosphere parallel to Tonga-Kermadec would produce a north-northeast axis of symmetry consistent with our simple sharp-gradient model. However, if the source of the anisotropic gradient lies beneath the lithosphere, the sensitivity of Love waves to *P* anisotropy is too weak to generate the observed waveforms; a sharp gradient of 2% *S*-wave anisotropy in the asthenosphere (depth range = 100 to 300 km) can model the observed quasi-Love waves adequately.
27. Earthquake locations and magnitudes are from the daily bulletins of the U.S. National Earthquake Information Center.
28. Data from several broadband seismic networks contributed to our study: the Global Digital Seismograph Network (GDSN), the Global Seismographic Network of the Incorporated Research Institutions for Seismology (IRIS), in cooperation with the International Deployment of Accelerometers (IDA) at the University of California, San Diego, and the U.S. Geological Survey, Project Geoscope, Mednet, and the Chinese Digital Seismic Network. Seismic data were obtained through the IRIS Data Management Center. The source mechanisms for the Landers and Balleny Islands earthquakes were provided by the Harvard centroid moment tensor Project, courtesy of G. Ekstrom and M. Salgalnik. D. M. Rye offered useful comments on the manuscript. Supported by NSF grant EAR-9018215.

18 March 1993; accepted 20 May 1993

Life History Variables Preserved in Dental Cementum Microstructure

Daniel E. Lieberman

The age and season of death of mammals, as well as other aspects of their life history, can be estimated from seasonal bands in dental cementum that result from variations in microstructure. Scanning electron micrographs of goats fed controlled diets demonstrate that cementum bands preserve variations in the relative orientation of collagen fibers that reflect changes in the magnitude and frequency of occlusal forces from chewing different quality diets. Changes in the rate of tissue growth are also reflected in cementum bands as variations in the degree of mineralization.

Cementum is an avascular, bone-like tissue that anchors tooth roots by mineralizing extrinsic collagen fiber bundles (Sharpey's fibers) produced in the periodontal ligament (*1, 2*). Cementum, which is continuously deposited and rarely remodeled or resorbed, grows in incremental bands (Fig. 1) that are visible in cross sections through tooth roots in polarized light or stained sections (*3*). Correlations between cementum bands and the age and season of death of mammals have been recognized for more than 30 years (*4–6*), but the underlying causes of the bands have been unknown. In most mammals, opaque acellular bands tend to be deposited during seasons of reduced tissue growth (such as winter), and translucent bands (cellular or acellular) tend to be deposited during seasons of rapid tissue growth (such as spring and summer) (*7–10*). In this report, I demonstrate that bands in cementum are caused by two different phenomena, occlusal strain and growth rate, that can be used to reconstruct significant life history variables of mammals after death.

Cementum has a complex three-dimensional microstructure that reflects its function to maintain teeth in position for effective occlusion in spite of the high strains caused by chewing (*11*). Scanning electron microscope (SEM) micrographs of fractured tooth roots (Fig. 2A) show that cementum microstructure is influenced principally by Sharpey's fiber orientation. Sharpey's fibers in cellular and acellular cementum tend to be oriented parallel to one another at an oblique angle relative to the dentine-cementum border. Sharpey's fibers in cementum are therefore aligned so as to counter the tensile forces that tend to depress teeth in their alveoli during occlusion. In addition, the predominant orientation of intrinsic collagen fibers within the cementum matrix is perpendicular to the Sharpey's fiber bundles (Fig. 2B). These fibers also appear to wrap around Sharpey's fibers (*13*). Cementum microstructure is thus analogous to other mineralized tissues, such as bone or tendon, in which collagen fibers are generally aligned at right angles to each other (*13–16*). However, unlike bone or tendon, cementum microstructure is determined primarily by extrinsic collagen.

I tested the effects of changes in diet on cementum microstructure in a controlled

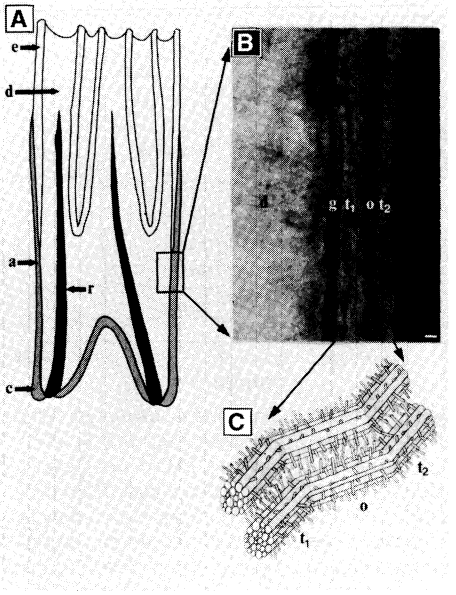

Fig. 1. Cross section of goat tooth showing location of tissues, increments, and collagen fiber orientation in increments. (**A**) Schematic cross section of lower first molar (M_1) showing location of enamel (e), dentine (d), acellular cementum (a), cellular cementum (c), and root canal (r). (**B**) Transmitted polarized light micrograph of ground section (50 μm thick) of M_1 from lingual surface near enamel-dentine-cementum junction. The goat was fed hard food for 4 months, soft food for 4 months, and hard food for 4 months. Dentine (d), first translucent increment corresponding to harder food diet for first 4 months (t_1), opaque increment corresponding to softer food diet for middle 4 months (o), second translucent increment corresponding to harder food diet for last 4 months (t_2), and granular layer of Tomes (the cementum-dentine border) (g). Tissue deposited during each phase was labeled with calcein (20 mg per kilogram of body weight), oxytetracycline (50 mg/kg), and alizarin red (50 mg/kg). Scale bar represents 10 μm. (**C**) Idealized reconstruction of collagen orientation in cementum bands in (B), depicting larger Sharpey's fiber bundles, which vary in orientation between bands, and the smaller fibers of intrinsic collagen that are aligned at right angles to the Sharpey's fibers. Sharpey's fiber bundles mineralized under conditions of higher bite force (increments t_1 and t_2) are more vertically oriented than those mineralized under conditions of lower bite force (increment o).

Department of Anthropology and the Society of Fellows, Harvard University, 11 Divinity Avenue, Cambridge, MA 02138.